

Phosgene-free decomposition of dimethylhexane-1,6-dicarbamate over ZnO

Min Jeong Hyun¹ · Mi Shin¹ · Yong Jin Kim² ·
Young-Woong Suh¹

Received: 11 July 2015 / Accepted: 11 August 2015
© Springer Science+Business Media Dordrecht 2015

Abstract In catalytic decomposition of dimethylhexane-1,6-dicarbamate (HDC) into hexamethylene-1,6-diisocyanate (HDI), Zn-containing homogeneous (i.e., zinc acetate) and heterogeneous (i.e., ZnO) catalysts were active among a number of catalysts tested, due to the great electron withdrawing ability of Zn ions. Particularly, when polyethylene glycol dimethyl ether was used as a solvent, ZnO was found to be relatively robust, because the catalytic performance was maintained up to the third use (HDC conversion of 93 % and HDI yield of 67 % at 180 °C for 1 h). Through investigation of a HDC/ZnO mixture at elevated temperatures by IR spectroscopy, a possible reaction scheme of ZnO-catalyzed decomposition of HDC was proposed. The H atom is removed from the N–H group of HDC by hydrogen bonding with an O site on the ZnO surface, followed by coordination of an O–C=O group in monodentate mode to a Zn site. The C–O group in the O–C=O linkage is then cleaved yielding the isocyanate and surface methoxide species. Finally, methanol is released from ZnO by a reaction between the surface methoxide and the hydroxyl species.

Keywords Catalytic decomposition · Hexamethylene-1,6-diisocyanate · Dimethylhexane-1,6-dicarbamate · ZnO

✉ Young-Woong Suh
ywsuh@hanyang.ac.kr

¹ Department of Chemical Engineering, Hanyang University, Seoul 133-791, Republic of Korea

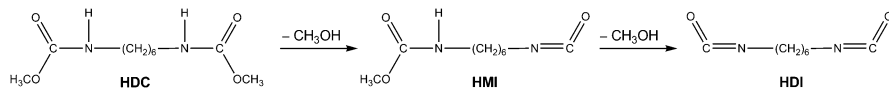
² Green Process Material Research Group, Korea Institute of Industrial Technology, Cheonan 331-822, Republic of Korea

Introduction

Diisocyanates are important intermediates in the manufacture of polyurethanes, where the typical chemicals are toluene diisocyanate (TDI) and methylene diphenyl diisocyanate (MDI) to produce flexible and rigid polyurethane foams, respectively [1]. In addition to aromatic diisocyanates, aliphatic ones such as hexamethylene diisocyanate (HDI) are useful for resistance to ultraviolet light and outdoor weathering, even though they are used in smaller volumes [2]. The global consumption of these diisocyanates has been gradually increasing due to higher demand in versatile commodity products including cushioning material in furniture and bedding, insulation material in construction and refrigeration, synthetic leather, etc.

Diisocyanates have been typically synthesized by the reaction of amines with phosgene or its derivatives. The phosgene route, however, has serious drawbacks such as handling of toxic feedstock and formation of corrosive HCl as a byproduct; thus, phosgene-free routes are now being developed in industry and academia [3, 4]. The reductive carbonylation of nitro compounds was introduced as a promising and sustainable pathway [3], but the presence of highly toxic residues in the final products was reported [5]. Additional attractive routes are the conversion to carbamates, including the reductive carbonylation in alcohols [6] and the other reaction of primary or secondary amine with dialkyl carbonates, particularly dimethyl carbonate [7]. Although the decomposition of carbamates into isocyanates is essential in both routes, few reports are yet available in the literature compared to the synthesis of carbamates.

Thermal decomposition of aryl- and alkyl-carbamates has to be conducted at high temperatures due to its endothermic reaction, resulting in the occurrence of many side reactions and the lower selectivity to the desired isocyanates. These problems can be overcome by an efficient catalyst operated at relatively lower temperatures. It has been reported that Zn-containing catalysts, such as zinc powder [8], zinc acetate [8], ZnO [9], Zn/ZnO [10], Zn-incorporated berlinite [7], and Bi-Zn composite oxide [11], as well as di-*n*-butyltin oxide [12, 13], montmorillonite K-10 [14, 15], and nano Cu₂O [16] are active in carbamate decomposition. Among these, ZnAlPO₄, Bu₂SnO, and K-10 catalysts were applied for decomposition of dimethylhexane-1,6-dicarbamate (HDC) into HDI, where the mono-isocyanate (HMI) is an intermediate formed by the decomposition of one carbamate end of HDC as follows [17]:



In this study, the catalyst screening work was conducted to find a highly active catalyst for HDC decomposition. Particularly, our attention was paid to the development of a heterogeneous catalyst due to its easy handling in separation and reuse. The effects of several reaction variables such as reaction solvent, temperature, and time were subsequently investigated in order to achieve the

highest HDI yield under the optimized reaction condition. The experiments for catalyst recycling were also carried out. Consequently, the change of characteristic amide bands of HDC in the absence or presence of the catalyst was investigated using infrared spectroscopy, thus proposing a possible reaction scheme.

Experimental

Chemicals and materials

HDI (99 %, TCI), nitrobenzene (99.5 %, Junsei), and polyethylene glycol dimethyl ether (avg. $M_n \approx 250$, Sigma-Aldrich) were purchased and used without purification. HDC was synthesized by the reaction of HDI with methanol at 50 °C for 6 h, where the methanol/HDI molar ratio was 10. The compound was finally obtained by purification, yielding the purity of >99 %, confirmed by ^1H NMR spectroscopy. Prior to use, the sample was kept in a vacuum desiccator.

Homogeneous catalysts used for catalyst screening were $\text{Ca}(\text{CH}_3\text{COO})_2 \cdot n\text{H}_2\text{O}$ (99 %, Sigma-Aldrich), $\text{Cr}(\text{CH}_3\text{COO})_2 \cdot n\text{H}_2\text{O}$ (95 %, Sigma-Aldrich), $\text{La}(\text{NO}_3)_3 \cdot 6\text{H}_2\text{O}$ (98 %, Junsei), $\text{Mg}(\text{CH}_3\text{COO})_2 \cdot 4\text{H}_2\text{O}$ (99 %, Sigma-Aldrich), $\text{Mn}(\text{CH}_3\text{COO})_2 \cdot 4\text{H}_2\text{O}$ (99 %, Yakuri), $\text{Ni}(\text{CH}_3\text{COO})_2 \cdot 4\text{H}_2\text{O}$ (98 %, Junsei), $\text{Zn}(\text{CH}_3\text{COO})_2 \cdot 2\text{H}_2\text{O}$ (99 %, Sigma-Aldrich), ZrCl_4 (98 %, Alfa Aesar), $\text{ZrOCl}_2 \cdot 8\text{H}_2\text{O}$ (98 %, Sigma-Aldrich), and $\text{ZrO}(\text{NO}_3)_2 \cdot n\text{H}_2\text{O}$ (100 %, Strem). These are used after pretreatment at 105 °C for 12 h. For heterogeneous catalysts, activated carbon (250–350 mesh, Yakuri), $\gamma\text{-Al}_2\text{O}_3$ (97 %, Strem), BaO (99.99 %, Sigma-Aldrich), and MgO (99.99 %, Sigma-Aldrich) were used as received. In case of zeolite catalysts, $\text{NH}_4\text{-ZSM-5}$ ($\text{SiO}_2/\text{Al}_2\text{O}_3 = 30$, CBV3024E, Zeolyst) was transformed into H-ZSM-5 by calcination at 600 °C for 3 h, while H-Y ($\text{SiO}_2/\text{Al}_2\text{O}_3 = 30$, CBV720, Zeolyst) and H-Beta ($\text{SiO}_2/\text{Al}_2\text{O}_3 = 28$, 931HOA, Tosoh) were pretreated at 500 °C with O_2 for 3 h.

Preparation of ZnO

ZnO catalyst was prepared by the precipitation method. In a typical preparation, an aqueous $\text{Zn}(\text{NO}_3)_2$ solution (1.0 M, 100 ml) was added with the rate of 5 ml/min into an aqueous NaHCO_3 solution (1.2 M, 200 ml) at 70 °C under vigorous stirring. After complete addition (final pH of about 7), the resulting precipitate suspension was stirred at the same temperature for 30 min and aged for 60 min. Then, the precipitate was filtered and washed with deionized water (ca. 1000 ml). The washing step was repeated at least three times in order to completely remove residual ions. The filter cake was dried in an oven at 105 °C overnight, crushed, and sieved for obtaining the particle size of smaller than 200 μm . Finally, the calcination was carried out in static air at 350 °C for 3 h.

Characterization

XRD analysis was conducted with a Rigaku D/Max RINT 2000 diffractometer using $\text{Cu K}\alpha$ ($\lambda = 0.1541 \text{ nm}$) as a radiation source (40 kV and 60 mA) in the 2θ range of

10°–90°. The infrared spectra of the samples were recorded using a Nicolet 6700 FT-IR spectrometer equipped with a MCT-A detector in the range of 4000–650 cm^{-1} with the resolution of 4 cm^{-1} . For the preparation of IR pellets, HDC was premixed with KBr and ZnO at the mixing weight ratio of 1/100 and 1/200, respectively, followed by pressing the sample (100 mg for HDC/KBr and 50 mg for HDC/ZnO) at 2700 psi for 90 s. The resulting pellet was loaded inside the IR cell (Specac HTHP cell with ZnSe windows) working in the transmission mode [18] and purged at an ambient temperature with N_2 (99.999 %, 50 ml/min) for 0.5–1 h. Finally, as the temperature was increased to 200 °C at the ramping rate of 5 °C/min under N_2 atmosphere, IR spectra were obtained at certain temperatures, where KBr and ZnO were used to take a background spectrum for HDC/KBr and HDC/ZnO pellets, respectively.

Activity test

The reaction was carried out in a three-neck round-bottom flask (100 ml) to which the reaction solvent (5 g) and HDC (0.5 g) were charged. Then, the reaction flask was purged with N_2 (99.999 %) at the flow rate of 150 ml/min for 30 min to make sure of the complete removal of inner oxygen and heated at the ramping rate of 10 °C/min. Note that any HDC is not lost at this purge step. As soon as the temperature approached the desired value, the catalyst of 30 mg was added to the reaction mixture and the reaction was started (reaction time = 0). Note that N_2 flow of 150 ml/min in the reaction flask was kept until the end of the reaction in order to continuously remove methanol produced by the decomposition of carbamate to isocyanate. After the reaction was complete, the sample (ca. 0.2 g) was taken out, filtered through a syringe filter (0.45 μm), and mixed with the GC calibration solvent *N*-methyl-2-pyrrolidone (NMP). This mixture was finally analyzed with a Younglin YL6500 GC equipped with a FID detector and an HP-5 column (30 m \times 0.25 mm \times 0.25 μm). Through quantitative measurements of HDC and HDI, the HDC conversion and HDI yield were calculated based upon the quantities of the converted HDC and the produced HDI. For calculating the HMI yield, the GC conversion factor (CF) of HDI was utilized assuming that the CF values of HMI and HDI were the same, since its authentic sample was not commercially available. In this case, the mole balance was measured to be almost near 100 % with the experimental error of ± 3 % at all reaction runs.

Results and discussion

Catalyst screening on the catalytic decomposition of HDC

For the conversion of HDC into the corresponding isocyanate at 160 °C, a number of catalysts, homogeneous or heterogeneous, were tested in this work (Fig. 1). Among homogeneous catalysts, zinc acetate ($\text{Zn}(\text{OAc})_2$) showed the best catalytic performance, where the yields of HMI and HDI were 41 and 17 %, respectively. Note that HMI is a more abundant product than HDI, meaning the facile

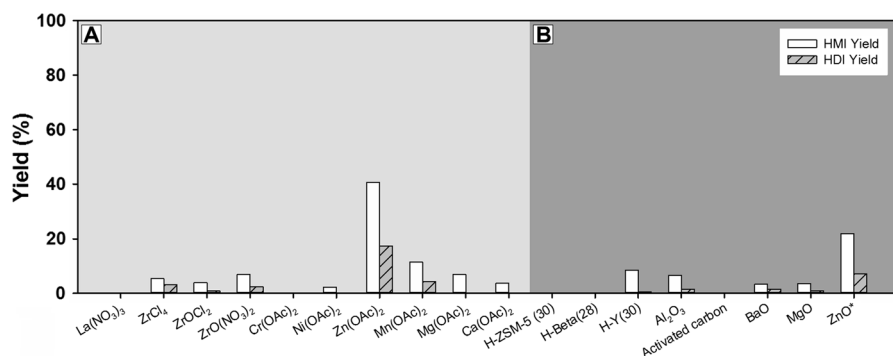


Fig. 1 Activities of homogeneous (a) and heterogeneous (b) catalysts tested for HDC decomposition at 160 °C. The asterisk stands for the use of 180 °C for ZnO catalyst

decomposition of HDC to mono-isocyanate rather than to diisocyanate. Thus, several homogeneous catalysts with an acetate ligand were applied for HDC decomposition; however, their catalytic activities were not superior to that of Zn(OAc)₂ (Fig. 1a). The activities of several heterogeneous catalysts were also investigated, in which their character depends upon acidity, basicity, and amphotericity. However, other catalysts except ZnO did not exhibit any noticeable isocyanate yields (Fig. 1b). The HMI and HDI yields were 22 and 7 % over ZnO, respectively. It should be noted here that the HDI selectivity was not high even if the reaction temperature of 180 °C was employed in order to compensate for lower activities of heterogeneous catalysts. The higher activities of Zn(OAc)₂ and ZnO are presumably due to greater electron withdrawing ability of Zn ions, which was similarly observed in the methoxycarbonylation of diamine with dimethyl carbonate [19, 20].

Effect of reaction variables on the catalytic decomposition of HDC

Since the above results were obtained using nitrobenzene as a solvent, a new reaction solvent would be required for enhancing the catalytic activity and producing the diisocyanate HDI. It was found from the literature that there are the two key properties of a reaction solvent in carbamate decomposition, that is, a high boiling point and a proton withdrawing (electron donating) character. The first property comes from the fact that the conversion of carbamate needs to be operated at elevated temperatures because it is an endothermic reaction [7], while the latter is associated with an E1CB mechanism in which the hydrogen atom is first removed from the N–H group of carbamate [21, 22]. Thus, we tested polyethylene glycol dimethyl ether (PGDE) as a solvent, since Yang et al. [23] proposed a favorable production of dimethyl carbonate from urea and methanol owing to both properties of PGDE (i.e., a high boiling electron donor). Figure 2 shows the activities of Zn(OAc)₂ and ZnO in nitrobenzene and PGDE, where HDC decomposition over the former and latter catalysts was conducted at 160 and 180 °C, respectively. Remarkably, the activities of both catalysts in PGDE were superior to those in

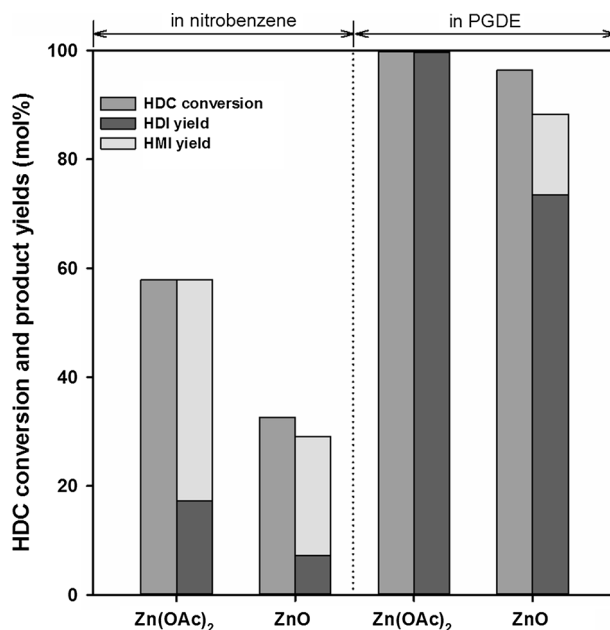


Fig. 2 Activity comparison of Zn(OAc)₂ and ZnO catalysts in the HDC decomposition using the solvent, nitrobenzene or PGDE for 1 h. The reaction temperature was 160 °C for Zn(OAc)₂ and 180 °C for ZnO

nitrobenzene, where the major product was HDI in PGDE over the two catalysts. Even in a blank experiment (i.e., without a catalyst) at 180 °C, PGDE exhibited the HDC conversion and HDI yield of 23 and 8 %, respectively, whereas any isocyanate products were not detected in nitrobenzene. This originates from the electron donor character of PGDE to abstract the H atom from the N–H group of carbamate. Therefore, it is believed that PGDE is a powerful solvent for efficient decomposition of HDC into the corresponding diisocyanate.

For further work, ZnO was chosen as a catalyst, although Zn(OAc)₂ showed the higher HDI yield. This is due to difficulty in the separation and reuse of homogeneous catalysts, as well as decomposition of acetate ligand above 160 °C observed by TGA. The effects of reaction variables (mainly, reaction temperature and time) were investigated for ZnO-catalyzed decomposition of HDC in PGDE. Figure 3 presents the HDC conversion and product yields obtained at the temperature of 160–200 °C, because the catalytic activity was hardly achieved below 160 °C and the mole balance at higher temperatures than 200 °C was far from 100 % due to occurrence of side reactions discussed below. At 160 °C, ZnO appeared to become active (HDC conversion = 28 %) with the HDI selectivity of 50 %. The activity of ZnO substantially increased at 180 °C affording the HDC conversion of 96 % and the total isocyanates yield of 89 % (74 % HDI and 15 % HMI). The difference between the two values was more evident at 200 °C (16 % = 100 % HDC conversion – 84 % HDI yield). This indicates further conversions of some isocyanates at higher temperatures, such as the self-addition of

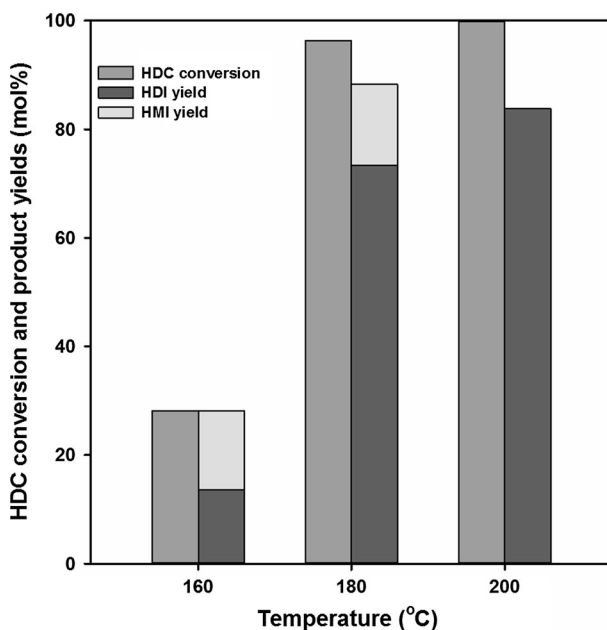


Fig. 3 Effect of reaction temperature on the HDC decomposition over ZnO catalyst in PGDE for 1 h

isocyanate (products: uretidinedione, isocyanurate, carbodiimide), condensations between unconverted carbamate and isocyanate (product: allophanate) and between carbodiimide and isocyanate (product: uretoneimine), and further polymerization [7]. Since polymerized products were visually observed inside the reactor after the reaction, a temperature higher than 200 °C should be avoided to produce HDI at the maximum yield.

The reaction progress of HDC decomposition over ZnO was monitored at 180 °C (Fig. 4). In an initial run, HMI and HDI were produced in similar amounts (22 and 20 % at 20 min, respectively). At little longer reaction periods, HDI was the major product because of the faster conversion of HMI into HDI than the initial HDC-to-HMI conversion in PGDE. The HDC conversion was complete and the HDI yield was close to 97 % at 2.5 h. When the experiment was conducted for more than 3 h, the HDI yield dropped to 85 % due to the above-mentioned side reactions. Therefore, the reaction time of 2–3 h is considered to be appropriate for the highest HDI yield.

Reusability of ZnO catalyst on the catalytic decomposition of HDC

The catalytic stability of ZnO was examined by recycling experiments under the condition such as 2 g HDC in 20 g PGDE, 0.133 g ZnO, 180 °C, and 1 h, which is a fourfold scale up than that used in the above sections for reproducibility and catalyst recovery. As shown in Fig. 5, the HDC conversion and HDI yield in the first run

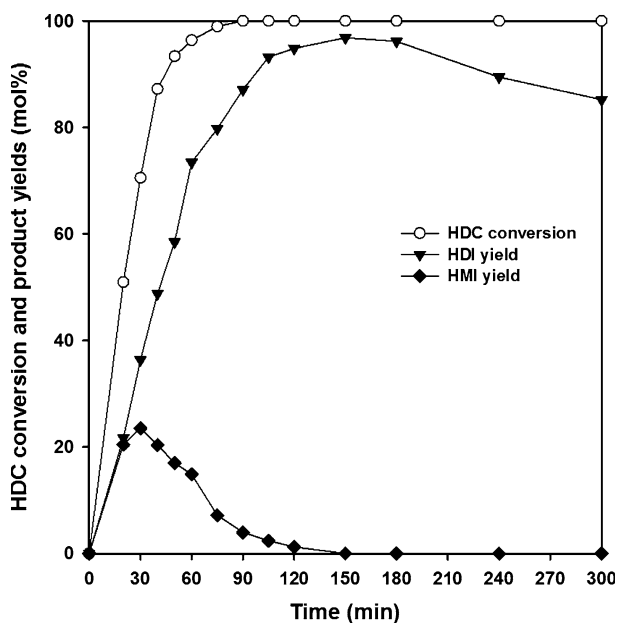


Fig. 4 Effect of reaction time on the HDC decomposition over ZnO catalyst in PGDE at 180 °C

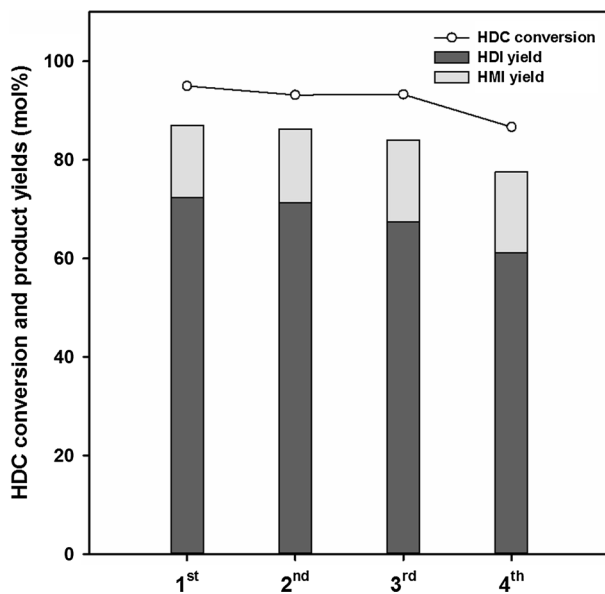


Fig. 5 Recycling test of ZnO catalyst on the HDC decomposition in PGDE. Reaction condition: HDC 2 g, PGDE 20 g, ZnO 0.133 g, 180 °C, and 1 h

were 95 and 72 %, respectively, where the HDI/HMI molar ratio was 4.9. Since the result is considered to be comparable to the previous data (HDC conversion of 96 % and HDI yield 74 %), the catalytic performance of ZnO appeared to be quite reproducible. Furthermore, the activity of ZnO was found to be maintained up to the third run, when the spent catalyst was recovered repeatedly through a series of operations including centrifugation, washing with methanol, and drying at 105 °C. However, the HDC conversion and HDI yield at the fourth run were decreased to 87 and 61 %, respectively, where the HDI/HMI molar ratio was 3.7. The apparent activity loss may be due to leaching of ZnO in some amounts into the reaction mixture and/or transformation of ZnO structure during recycling experiments.

In order to investigate the change of ZnO crystals during recycling experiments, XRD analysis was conducted for fresh and spent ZnO catalysts. Figure 6 presents XRD patterns of the fresh ZnO, and the spent ZnO catalysts obtained after the first and fourth runs. Evidently, all the reflections were identical to those of ZnO (JCPDS PDF No. 36-1451). Two kinds of differences were, however, observed in the spent catalysts: the intensities of major reflections of ZnO were lower and the baseline hump was seen at $2\theta = 21^\circ$. These findings suggest that a certain amount of crystalline ZnO is transformed into an amorphous form and subsequently leached out into the reaction mixture.

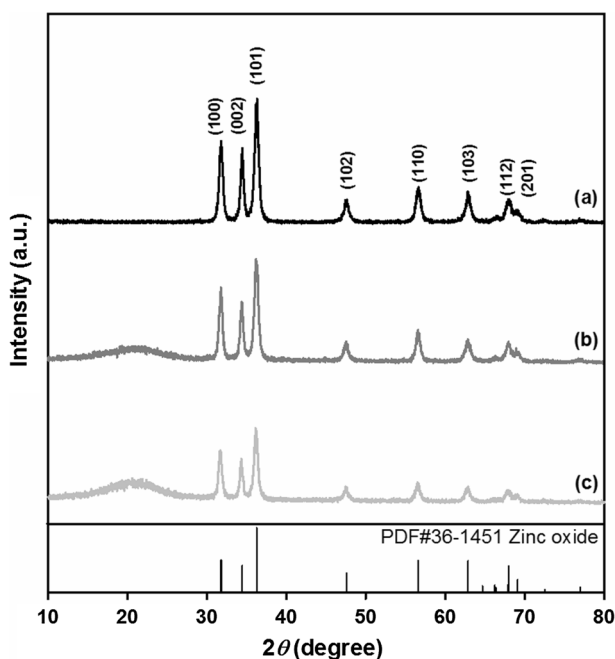


Fig. 6 XRD patterns of fresh ZnO (a) and spent ZnO obtained after the first (b) and fourth (c) runs

Plausible reaction mechanism for ZnO-catalyzed HDC decomposition

Amide bands of HDC were investigated by FT-IR spectroscopy, where HDC was pressed with KBr that had no catalytic activity on this reaction (Fig. 7a). Several characteristic bands were observed at 30 °C; 3340 cm^{-1} for amide A ($\nu(\text{N-H})$), 1693 cm^{-1} for amide I ($\nu(\text{C=O})$), 1537 cm^{-1} for amide II ($\delta(\text{N-H})$, $\nu(\text{C-N})$), 1264 cm^{-1} for amide III ($\delta(\text{N-H})$, $\nu(\text{C=O})$, $\nu(\text{C-N})$), 1195 and 1053 cm^{-1} for urethane ($\nu(\text{C-N})$, $\nu(\text{C=O})$, $\delta(\text{C-O-C})$). These frequency values were similar within the frequency difference of 1–4 cm^{-1} to those of a crystal HDC reported by Suchkova and Maklakov [24]. Upon heating the sample in N_2 flow to 200 °C, blue or red shifts occurred in these amide bands (blue: amide A and amide I, red: amide II and amide III). This is caused by dissociation of hydrogen bonds at elevated temperatures. The typical example is variation of amide A band with increasing the temperature. The intensity of the 3354 cm^{-1} absorption peak assigned to the bonded N-H group decreased and, simultaneously, that of the 3443 cm^{-1} absorption peak assigned to the free N-H group increased, as observed in *N*-hexyl hexyl carbamate [25]. This is an indication of a thermal effect on hydrogen bonding of HDC.

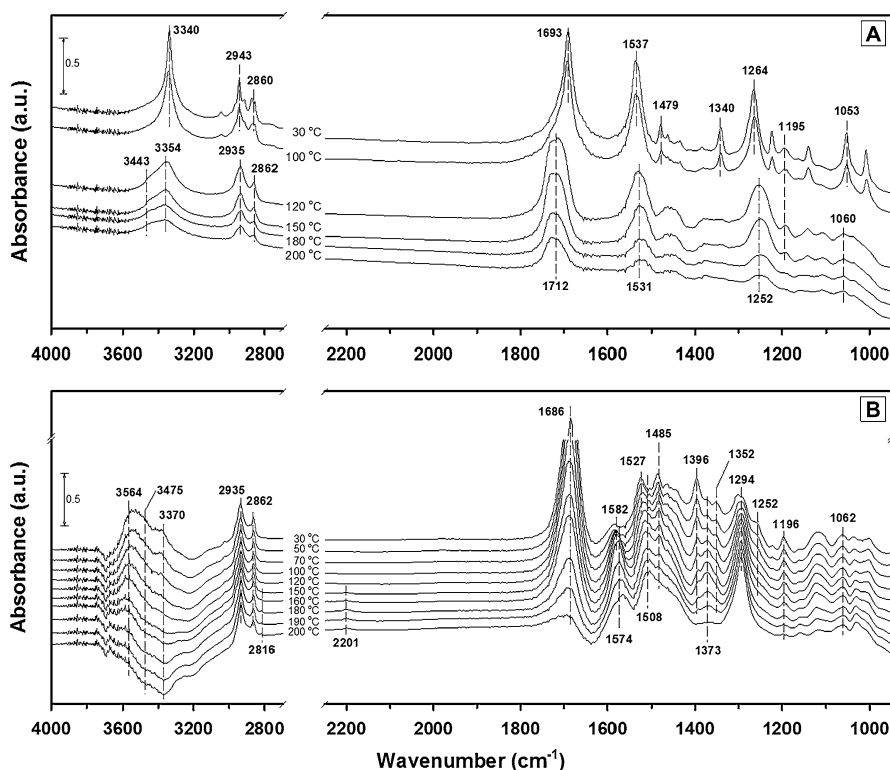


Fig. 7 FT-IR spectra obtained by heating pure HDC (a) and a mixture of HDC and ZnO (b) from 30 to 200 °C (ramping rate: 5 °C/min)

A mixture of HDC and ZnO was also characterized with increasing the temperature up to 200 °C (Fig. 7b). Compared to pure HDC, the absorption of amide A (3370 cm^{-1}), II (1527 cm^{-1}) and III (1252 cm^{-1}) bands were much diminished, relative to that of the amide I band (1686 cm^{-1}), in the spectrum recorded at 30 °C. Since these bands are all associated with the N–H group of HDC, the N–H bonding was presumed to be weakened due to interaction with ZnO. This is in accordance with appearance of new bands at 3564 and 3475 cm^{-1} , because Noei et al. [26] ascribed the bands to hydroxyl species ($\text{N-H}\cdots\text{O}$) formed by interaction of the N–H group with oxygen sites of the ZnO surface. Therefore, it is believed that the N–H group of HDC is coordinated via the H atom to the O site of the ZnO surface at 30 °C.

Upon heating the HDC/ZnO mixture to 200 °C, remarkable changes were observed. (1) The intensity of the amide A band at 3370 cm^{-1} and those of the bands at 3564 and 3475 cm^{-1} became negative. (2) The absorption bands at 1485 , 1396 , and 1352 cm^{-1} , related with δ_{as} or $\delta_{\text{s}}(\text{C-N-H})$ and $\nu(\text{C-N})$ [27], gradually decreased. These changes are explained by complete cleavage of N–H bonding of HDC and disappearance of the hydroxyl species formed on the ZnO surface. (3) The absorption of the amide I band at 1686 cm^{-1} was not shifted while the intensity was decreasing. When compared to the same band of pure HDC, the frequency difference was only 6 cm^{-1} . This implies no interaction of the C=O group of HDC with ZnO. (4) The absorption bands at 1582 and 1373 cm^{-1} grew up to 160 °C and then disappeared around 190–200 °C. From IR spectra of CO_2 -adsorbed ZnO samples [28, 29], these are considered to be a consequence of carboxylate binding with Zn sites: 1582 and 1373 cm^{-1} are assigned to $\nu_{\text{as}}(\text{O-C=O})$ and $\nu_{\text{s}}(\text{O-C=O})$, respectively. Also, the $\Delta\nu$ ($=\nu_{\text{as}}(\text{O-C=O}) - \nu_{\text{s}}(\text{O-C=O})$) of 209 cm^{-1} indicates monodentate coordination, because a larger $\Delta\nu$ value than 180 cm^{-1} is typical for this type of carboxylate binding mode [30]. Therefore, it can be suggested that the O–C=O group of HDC is coordinated in monodentate mode via the O atom of the C–O group to the Zn site of the ZnO surface at higher temperatures to 160 °C. Above this temperature, however, this binding will lessen (5). New absorption bands at 2201 and 2816 cm^{-1} were observed in the temperature range of 150–200 °C. For clarification, the spectra in the region $2900\text{--}2100\text{ cm}^{-1}$ were shown in Fig. 8. The former band suggests formation of isocyanate species on ZnO. Guglielminotti and Boccuzzi [31] observed a band at 2205 cm^{-1} assigned to an isocyanate group formed by adsorption of NO and CO on Ru/ZnO. This is a direct evidence to show the transformation of the carbamate group of HDC into isocyanate on ZnO in this temperature range where the activity tests were conducted. On the other hand, the latter frequency is assigned to $\nu_{\text{s}}(\text{C-H})$ of CH_3O adsorbate, which was confirmed by exposure of methanol vapor on ZnO [32]. This means the cleavage of the C–O bond in the O–C=O linkage leaving the methoxide (CH_3O) species on the ZnO surface. Therefore, the observation of these two bands suggests that the carbamate group of HDC is decomposed to isocyanate over ZnO at 150–200 °C. (6) At 200 °C, the spectrum of the HDC/ZnO mixture was very similar to that of ZnO.

From the aforementioned FT-IR observations, a possible reaction scheme on ZnO-catalyzed decomposition of carbamate was proposed, as depicted in Fig. 9.

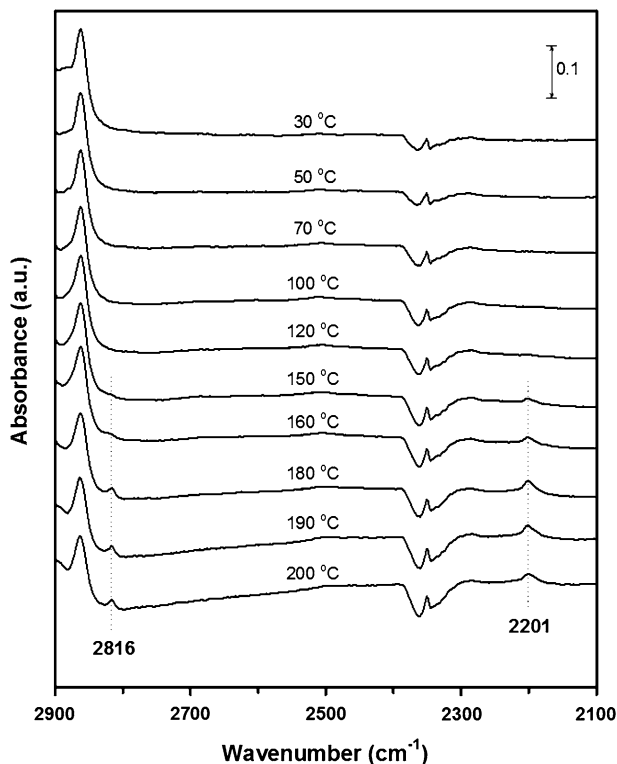


Fig. 8 Enlarged version of Fig. 7b in the region of 2900–2100 cm^{-1}

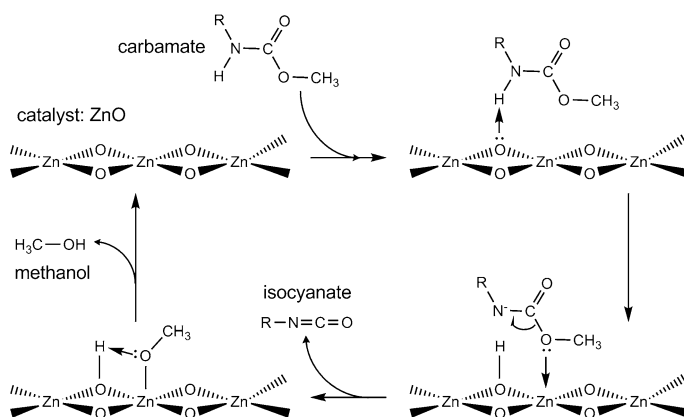


Fig. 9 Possible reaction scheme on ZnO-catalyzed decomposition of carbamate to isocyanate

The H atom is first removed from N–H group by hydrogen bonding with the O site of the ZnO surface, indicating that the decomposition follows an E1CB mechanism. Then, the O–C=O group is coordinated in the monodentate mode to the Zn site with

an electron withdrawing character. The C–O group in the O–C=O linkage is subsequently cleaved yielding an isocyanate product. The resulting surface methoxide species linked to Zn reacts with the H atom of the surface hydroxyl species, finally releasing methanol from ZnO.

Conclusion

We have elucidated the method to efficiently decompose HDC to HDI. Catalyst screening experiments revealed that Zn-containing catalysts $\text{Zn}(\text{OAc})_2$ and ZnO were highly active in the reaction due to the electron withdrawing character of Zn species. Furthermore, the HDC conversion and HDI yield of the two catalysts were enhanced using electron-donor PGDE as a solvent. From optimization works over ZnO selected due to thermal instability of $\text{Zn}(\text{OAc})_2$, the reaction condition of 180–200 °C and 2–3 h was appropriate for the highest HDI yield. Additionally, ZnO was found to be recyclable up to the third use. FT-IR results at elevated temperatures indicated the removal of the H atom from the N–H group of carbamate by interaction with the O site of the ZnO surface, the monodentate coordination of the O–C=O linkage to the Zn site, and the cleavage of the C–O group in O–C=O linkage yielding the isocyanate product and surface methoxide species that will be released into methanol from ZnO, thus suggesting a possible reaction scheme. Although the explanation was developed from results using HDC as the reactant, it should apply to other aliphatic carbamates since the structural and chemical characters of ZnO are important factors for decomposition performance.

Acknowledgments This research was supported by the Fusion Research Program for Green Technologies through the National Research Foundation of Korea (NRF) funded by the Ministry of Science, ICT & Future Planning (2012M3C1A1054501).

References

1. Z. Wirpsza, *Polyurethanes: Chemistry, Technology, and Applications* (Ellis Horwood, London, 1993)
2. M. Szycher, *Szycher's Handbook of Polyurethanes*, 2nd edn. (CRC Press, New York, 2012)
3. O. Kreye, H. Mutlu, M.A.R. Meier, *Green Chem.* **15**, 1431–1455 (2013)
4. H. van den Berg, L. van der Ham, H. Gutierrez, S. Odu, T. Roelofs, J. de Weerd, *Chem. Eng. J.* **207–208**, 254–257 (2012)
5. E. Drent, P.W.N.M. van Leeuwen, EP Patent 86281 (1983)
6. D. Chaturvedi, *Tetrahedron* **68**, 15–45 (2012)
7. D.-L. Sun, J.-Y. Luo, R.-Y. Wen, J.-R. Deng, Z.-S. Chao, *J. Hazard. Mater.* **266**, 167–173 (2014)
8. X. Zhao, Y. Wang, S. Wang, H. Yang, J. Zhang, *Ind. Eng. Chem. Res.* **41**, 5139–5144 (2002)
9. D. Chen, L.-M. Liu, Y. Wang, J. Yao, G.-Y. Wang, S.-X. Li, Y. Xue, J.-H. Zhan, *Chin. J. Catal.* **26**, 987–992 (2005)
10. X. Guan, H.Q. Li, H.T. Liu, F. Guo, X.X. Yao, *J. Beijing Univ. Chem. Technol. (Nat. Sci.)* **36**, 12–16 (2009)
11. Y. Dai, Y. Wang, Q. Wang, G. Wang, *Chin. J. Catal.* **30**, 1131–1136 (2009)
12. M. Takahito, A. Kyoji, K. Yasushi, JP Patent 6239826 (1994)
13. Y.-S. Dai, Y. Wang, J. Yao, Q.-Y. Wang, L.-M. Liu, L.-L. Cui, Y.-F. Zhao, G.-Y. Wang, *Acta Chim. Sin.* **65**, 1064–1070 (2007)
14. P. Uriz, M. Serra, P. Salagre, S. Castillon, C. Claver, E. Fernandez, *Tetrahedron Lett.* **43**, 1673–1676 (2002)

15. C.M. Serglo, C.C. Cannen, US Patent 6639101 (2003)
16. Q. Wang, W. Kang, Y. Zhang, X. Yang, J. Yao, T. Chen, G. Wang, *Chin. J. Catal.* **34**, 548–558 (2013)
17. X. Li, H. Li, H. Liu, G. Zhu, *J. Hazard. Mater.* **198**, 376–380 (2011)
18. J. Ryczkowski, *Catal. Today* **68**, 263–381 (2001)
19. T. Baba, A. Kobayashi, Y. Kawanami, K. Inazu, A. Ishikawa, T. Echizenn, K. Murai, S. Aso, M. Inomata, *Green Chem.* **7**, 159–165 (2005)
20. D.-L. Sun, J.-R. Deng, Z.-S. Chao, *Chem. Cent. J.* **1**, 27–35 (2007)
21. B.M. Bergon, N.B. Hamida, J.-P. Calmon, *J. Agric. Food Chem.* **33**, 577–583 (1985)
22. M.B. Berezin, O.M. Chernova, P.A. Shatunov, N.A. Pashanova, D.B. Berezin, A.S. Semeikin, *Molecules* **5**, 809–815 (2000)
23. B. Yang, D. Wang, H. Lin, J. Sun, X. Wang, *Catal. Commun.* **7**, 472–477 (2006)
24. G.C. Suchkova, L.I. Maklakov, *Vib. Spectrosc.* **51**, 333–339 (2009)
25. Q. Li, H. Zhou, D.A. Wicks, C.E. Hoyle, D.H. Magers, H.R. McAlexander, *Macromolecules* **42**, 1824–1833 (2009)
26. H. Noei, H. Qiu, Y. Wang, E. Löffler, C. Wöll, M. Muhler, *Phys. Chem. Chem. Phys.* **10**, 7092–7097 (2008)
27. D.-L. Sun, S.-J. Xie, J.-R. Deng, C.-J. Huang, E. Ruckenstein, Z.-S. Chao, *Green Chem.* **12**, 483–490 (2010)
28. G. Busca, V. Lorenzelli, *Mater. Chem.* **7**, 89–126 (1982)
29. S. Matsushita, T. Nakata, *J. Chem. Phys.* **36**, 665–669 (1962)
30. V. Zelenák, Z. Vargová, K. Györyová, *Spectrochim. Acta A* **66**, 262–272 (2007)
31. E. Guglielminotti, F. Boccuzzi, *J. Catal.* **141**, 486–493 (1993)
32. R.N. Spitz, J.E. Barton, M.A. Barteau, R.H. Staley, A.W. Sieight, *J. Phys. Chem.* **90**, 4067–4075 (1986)